

Compact Wideband Bandpass Filter Using Improved Triple-Mode Resonator with Broad Upper Stopband

Daotong Li¹, Yonghong Zhang¹, Kaida Xu², Kaijun Song¹, and Joshua Le-Wei Li³

¹ EHF Key Lab of Science

University of Electronic Science and Technology of China (UESTC), Chengdu 611731, China
bzxy06@gmail.com, zhangyhh@uestc.edu.cn, ksong@uestc.edu.cn

² Institute of Electromagnetics and Acoustics, Department of Electronic Science
Xiamen University, Xiamen 361005, China
xukaida25@gmail.com

³ Institute of Electromagnetics, School of Electronic Engineering
University of Electronic Science and Technology of China (UESTC), Chengdu 611731, China
lwli@uestc.edu.cn

Abstract — A triple-mode microstrip square ring short stub-loaded stepped impedance resonator (SIR) is proposed for the design of bandpass filters (BPFs). The resonator possesses three resonances over the wide frequency band, which can be employed to implement a BPF with flat response. This kind of the filter is able to control spurious response by changing the structure of the resonator. For validation, a triple-mode BPF with central frequency of 2.55 GHz has been designed, fabricated and measured. Good agreement is observed between measured and simulated results.

Index Terms — Triple-mode resonator, wideband bandpass filter, wide stopband response.

I. INTRODUCTION

With the rapid development of modern mobile and wireless communication systems, the filters with compact size and high performance are increasingly essential. Many ways have been developed to make the filters more compact. An effective one is to modify the traditional resonator to generate additional modes, thus the resonator can be treated as multiple resonators in electrical [1]. Among them, dual-mode filter is the most common multiple-mode filter, which has been analyzed deeply and comprehensively in many reports with various configurations, including circular loop [2], square loop [3], hexagonal loop [4], circular patch [5], defected ground structure [6], and triangular patch [7]. Triple-mode characteristics can be achieved by loading a stub to a resonator [8]. The $\lambda/2$ transmission line resonator with a pair of center loaded stubs is used to

design the triple-mode filters [9-10].

In this paper, we will present a different type of triple-mode filter by using a novel improved tri-section stepped impedance multiple-mode resonator. The multiple-mode resonator is developed from a conventional SIR dual-mode resonator [11]. By introducing a short stub and a square ring stub loaded in the center of the SIR, a compact triple-mode BPF with wideband response, wide stopband, low insertion loss, and high selectivity is realized. The proposed BPF has been simulated, implemented, and measured. Good agreement is observed between simulated results and measured results.

II. ANALYSIS AND DESIGN OF PROPOSED WIDEBAND BANDPASS FILTER

A. Characteristic of the triple-mode resonator

The proposed triple-mode resonator shown in Fig. 1 is excited via capacitive couplings by input/output port. It consists of a square ring, short stub and a SIR resonator, and the parameters are indicated in Fig. 1. Mode decomposition provides a deeper insight to the operation of the resonator, where the corresponding even- and odd-mode resonators are illustrated in Fig. 2.

The symmetrical plane in Fig. 1 will behave as an electric wall (EW) or a magnetic wall (MW) under the odd-mode or the even-mode excitation, respectively. The resonator equivalent circuits are depicted in Fig. 2, where Y_{ineven} and Y_{inodd} represent the input admittances of the odd-mode equivalent circuit and the even-mode equivalent circuit, respectively.

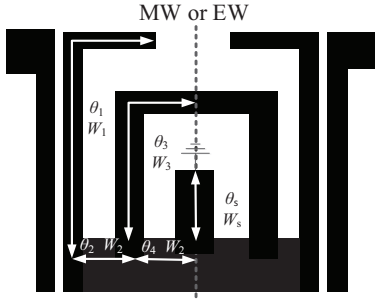


Fig. 1. Layout of proposed triple-mode resonator.

For even-mode excitation, the equivalent circuit is shown in Fig. 2 (a), which contains two resonant circuits: a tri-section quarter-wavelength resonator with one short end and a tri-section quarter-wavelength resonator with open end, as shown in Figs. 2 (c) and (e). The input impedance of the two even-mode equivalent circuits Y_{ineven_1} and Y_{ineven_2} can be deduced as:

$$Y_{ineven_1} = \frac{Z_1 Z_2 - Z_1 Z_3 \tan(\theta_3) \tan(\theta_2)}{j(Z_1 Z_2 Z_3 \tan(\theta_3) + Z_1^2 Z_2 \tan(\theta_2))} \quad (1.1)$$

$$\frac{-Z_2 Z_3 \tan(\theta_1) \tan(\theta_3) - Z_2^2 \tan(\theta_2) \tan(\theta_1)}{+Z_1 Z_2^2 \tan(\theta_1) - Z_1^2 Z_3 \tan(\theta_1) \tan(\theta_2) \tan(\theta_3)},$$

$$Y_{ineven_2} = \frac{-jZ_1 Z_2 Z_3 \cot \theta_1 + jZ_2^2 Z_3 \tan \theta_2}{Z_2 Z_3 + Z_1 Z_3 \cot \theta_1 \tan \theta_2} \quad (1.2)$$

$$\frac{+Z_2 jZ_3^2 \tan \theta_3 + jZ_1 Z_3^2 \cot \theta_1 \tan \theta_3 \tan \theta_2}{+Z_1 Z_2 \cot \theta_1 \tan \theta_3 - Z_2^2 \tan \theta_2 \tan \theta_3},$$

where θ_i ($i=1,2,3$ and s) is the electrical length for the section of the triple-mode resonator shown in Fig. 2.

The two even-mode resonance condition can be derived by setting $Y_{ineven_1} = 0$ and $Y_{ineven_2} = 0$. Figure 2 (c) shows the Path I of even-mode equivalent circuit. The resonant frequencies of f_{even_2} can be extracted as follows:

$$\frac{Z_3}{Z_2} \tan(\theta_2) \tan(\theta_3) + \frac{Z_3}{Z_1} \tan(\theta_1) \tan(\theta_3) \quad (1.3)$$

$$+ \frac{Z_2}{Z_1} \tan(\theta_1) \tan(\theta_2) = 1.$$

For the simplicity of analysis, keep the condition of $\theta_1 = \theta_2 = \theta_3 = \theta$, and set $K_1 = Z_1/Z_2$, $K_2 = Z_2/Z_3$, then (1.3) can be rewritten as:

$$\left(\frac{1}{K_2} + \frac{1}{K_1 K_2} + \frac{1}{K_1} \right) \tan^2(\theta) = 1. \quad (1.4)$$

Therefore, the condition for the fundamental resonance of a symmetrical tri-section SIR with equal section lengths can be derived as [12-13]:

$$\theta = \tan^{-1} \left(\sqrt{\frac{K_1 K_2}{K_1 + K_2 + 1}} \right). \quad (1.5)$$

Similarly for the resonant frequencies of f_{even_1} , Fig. 2 (e) shows the Path II of even-mode equivalent circuit. When $\theta_1 = (\theta_2 + \theta_4) = \theta_s = \theta$ and $K_3 = Z_2/Z_s$, the fundamental resonant frequency f_{even_1} occurs at:

$$\theta = \tan^{-1} \left(\sqrt{\frac{K_1 + K_1 K_3 + 1}{K_3}} \right). \quad (1.6)$$

For odd-mode excitation, its equivalent circuit shown in Fig. 2 (b) can be decomposed into two resonant circuits: a tri-section stepped-impedance resonators and a quarter-wavelength SIR, which are shown in Figs. 2 (d) and (e), respectively. The required odd-mode resonant frequency f_{odd_1} is introduced by the typical quarter-wavelength SIR. The input impedance of the two odd-mode equivalent circuit Y_{inodd_1} can be deduced as:

$$Y_{inodd_1} = \frac{Z_2 - Z_1 \tan(\theta_1) \tan(\theta_2 + \theta_4)}{jZ_2 ((Z_1 \tan(\theta_1) + Z_2 \tan(\theta_2 + \theta_4)))}. \quad (1.7)$$

The resonance condition can be derived by setting $Y_{inodd_1} = 0$. The fundamental resonant frequency f_{odd_1} occurs at:

$$\tan(\theta_1) \tan(\theta_2 + \theta_4) = K_1. \quad (1.8)$$

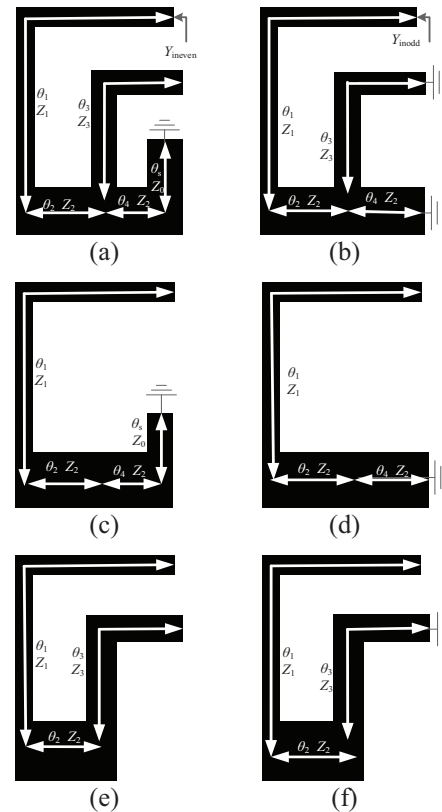


Fig. 2. Equivalent circuits of the triple-mode resonator: (a) even-mode, (b) odd-mode, (c) Path I of even-mode equivalent circuit, (d) Path I of odd-mode equivalent circuit, (e) Path II of even-mode equivalent circuit, and (f) Path II of odd-mode equivalent circuit.

Figure 3 shows the EM simulated frequency responses of the triple-mode resonator under the weak coupling, where f_i ($i=1, 2$ and 3) corresponds to the i th resonant frequency of triple-mode resonator and f_{zi} ($i=1$ and 2) are the frequency locations of the transmission zeros. We can see that there are three resonances in the passband of the filter and two transmission zeros near the passband edges.

Figure 4 shows the simulated even- and odd-mode normalized resonant frequencies f_i/f_0 , where f_0 is set to 2.35 GHz. It is obvious to see from Figs. 4 (a), (b) that the resonant frequency f_{odd_1} receives little influence from the introduced square ring and short-stub, whereas f_{even_1} and f_{even_2} can be varied separately by changing the length θ_s and L_3 of the short-stub and square ring, respectively. As shown in Fig 4 (a), by changing the short-stub length θ_s , the first resonant frequency f_{even_1} can be shifted within a wide range, while the f_{odd_1} is fixed and f_{even_2} varies slightly. Figure 4 (b) shows the distribution of resonant frequencies for cases of different length of θ_3 , it is clear that the third resonant frequency f_{even_2} can be shifted within a wide range, while f_{even_1} and f_{odd_1} are nearly unchanged.

According to the curves in Fig. 5, the variation of resonant frequencies can be controlled by changing the impedance ratios of the tri-section SIR. As shown in Fig. 5 (a), the resonant frequency f_{even_1} can be changed widely by altering the impedance ratio of K_3 , and the resonance frequencies f_{odd_1} and f_{even_2} varies slightly. It also can be seen from Fig. 5 (b), the resonant frequency f_{even_2} can be shifted within a wide range versus different impedance ratio of K_2 , with the resonant frequencies f_{even_1} and f_{odd_1} having almost no change. Figure 5 (c) shows the variation of resonant frequencies f_{even_1} , f_{odd_1} and f_{even_2} versus the impedance ratio of K_1 , which have a common trend, but the change of resonant frequency f_{odd_1} is more intense.

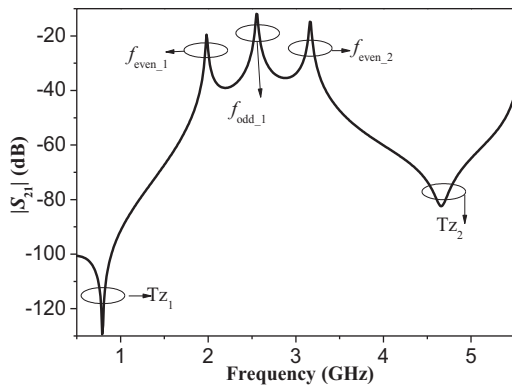


Fig. 3. Simulation transmission response of the wideband filter with weak coupling.

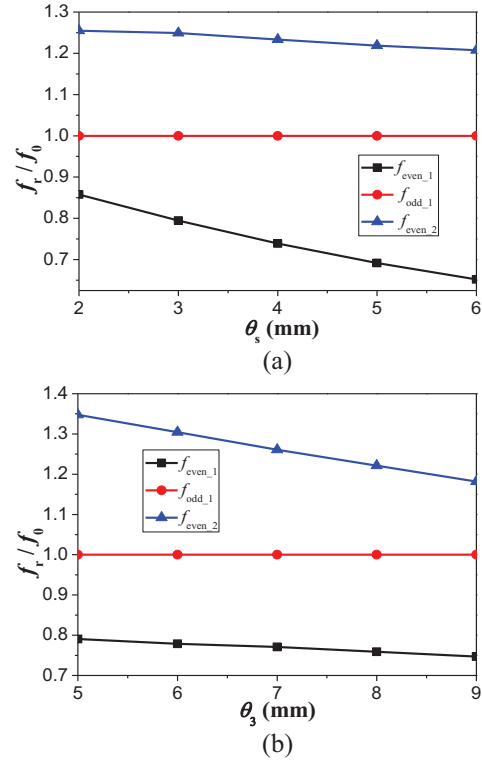
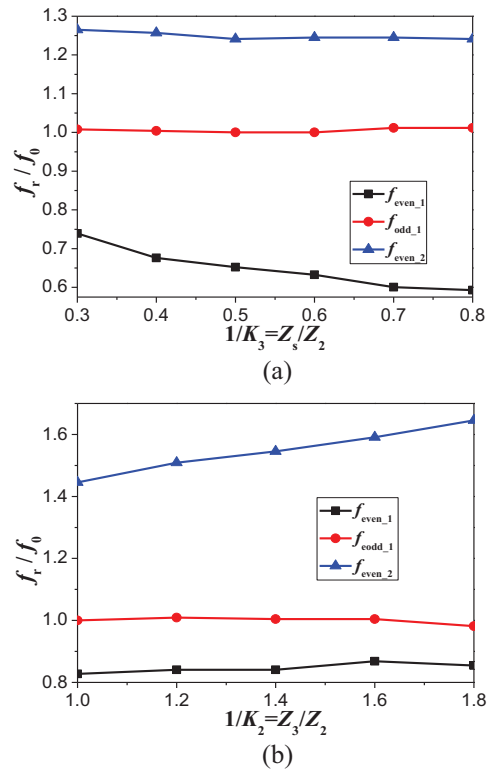


Fig. 4. (a) Analysis of resonator frequencies versus θ_s , and (b) analysis of resonator frequencies versus θ_3 .



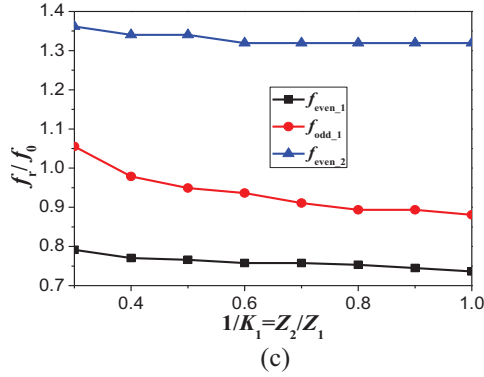


Fig. 5. Variation of resonant frequencies versus impedance ratio. Analysis of resonator frequencies versus impedance ratio of: (a) K_3 , (b) K_2 , and (c) K_1 .

Based on the above analysis, the resonant frequencies of the proposed triple-mode resonator could be controlled by tuning the length of θ_1 , θ_2 , θ_3 and θ_s and the impedance ratio K_1 , K_2 and K_3 . There is more freedom in design compared with traditional triple-mode resonator.

B. Filter design

The coupling scheme of the triple-mode filter is presented in Fig. 6. The dark circles and the white circles indicate resonant modes of resonators and source/load, respectively. These modes are all directly coupled to both the source and the load. The coupling between microstrip resonator and source/load can be modified by changing their distance and overlap length. The coupling between the even mode of the triple-mode resonator and input or output are both positive and the coupling between the odd mode and source is positive, while the coupling between this mode and load is negative. The dashed line indicates the coupling between source and load that is determined by the gap between input and output microstrip line. Therefore, the corresponding coupling matrix of the coupling scheme is given by:

$$M = \begin{bmatrix} 0 & M_{S1} & M_{S2} & M_{S3} & M_{SL} \\ M_{1S} & M_{11} & 0 & 0 & M_{1L} \\ M_{2S} & 0 & M_{22} & 0 & M_{2L} \\ M_{3S} & 0 & 0 & M_{33} & M_{3L} \\ M_{LS} & M_{L1} & M_{L2} & M_{L3} & 0 \end{bmatrix} \quad (1.9)$$

Due to symmetrical geometry of the proposed filter, the coupling coefficients agree with $M_{S1}=M_{L1}$, $M_{S2}=M_{L2}$, and $M_{S3}=-M_{L3}$. So two inherent transmission zeros of the resonator and a transmission zero introduced by the source-load coupling can be achieved, which improve the selectivity of the proposed BPF. Therefore, the generalized coupling matrix for the proposed BPF with

central frequency of 2.55 GHz can be obtained on the basis of the approach of synthesis in [14] as follows:

$$M = \begin{bmatrix} 0 & -0.6042 & -0.4861 & 0.8205 & 0.0186 \\ -0.6042 & 1.5887 & 0 & 0 & 0.6035 \\ -0.4861 & 0 & -1.4814 & 0 & 0.4854 \\ 0.8205 & 0 & 0 & -0.2436 & 0.8199 \\ 0.0186 & 0.6035 & 0.4854 & 0.8199 & 0 \end{bmatrix}$$

The scattering characteristic of the proposed filter shown in Fig. 7 was synthesized. Three transmission poles are clearly observed in the passband of the filter. In addition, three transmission zeros are created which improve the selectivity in the transition band and rejection in the stopband.

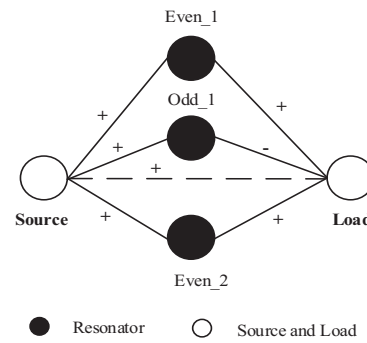


Fig. 6. The coupling scheme of proposed triple-mode BPF.

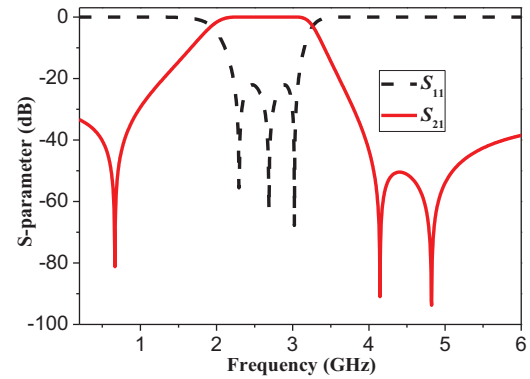


Fig. 7. Synthesized theory result of triple-mode BPF.

III. SIMULATION AND EXPERIMENT

Based on the triple-mode resonator, a wide-band BPF has been designed and fabricated on Taconic RF-35 substrate with relative dielectric constant of $\epsilon_r=3.5$ and thickness of $h=0.508$ mm. The geometry of the proposed filter is shown in Fig. 8. It consists of one triple-mode resonator and a pair of parallel-coupled quarter wavelength feedlines. The dimensions of the proposed wideband BPF shown in Fig. 8.

- vol. 52, pp. 1237-1243, 2004.
- [8] J. S. Hong and H. Shaman, "Dual-mode microstrip open-loop resonators and filters," *IEEE Trans. Microw. Theory Tech.*, vol. 55, pp. 2099-2109, 1996.
- [9] L. Zhu and W. Menzel, "Compact microstrip bandpass filter with two transmission zeros using a stub-tapped half wavelength line resonator," *IEEE Microw. Wireless Compon. Lett.*, vol. 13, pp. 16-18, 2003.
- [10] L. Li, Z.-F. Li, and Q.-F. Wei, "A quasi-elliptic wideband bandpass filter using a novel multiple-mode resonator constructed by an asymmetric compact microstrip resonant cell," *Microw. Opt. Technol. Lett.*, vol. 51, pp. 713-714, 2009.
- [11] M. Makimoto and S. Yamashita, "Bandpass filters using parallel coupled stripline stepped impedance resonators," *IEEE Trans. Microw. Theory Tech.*, vol. 28, pp. 1413-1417, 1980.
- [12] D. Packiaraj, M. Ramesh, and A. T. Kalghatgi, "Design of a tri-section folded SIR filter," *IEEE Microw. Wireless Compon. Lett.*, vol. 16, pp. 317-319, 2006.
- [13] A. Eroglu and R. Smith, "Triple band bandpass filter design and implementation using SIRs," *26th Annual Review of Progress in Applied Computational Electromagnetics (ACES)*, pp. 862-865, Tampere, Finland, Apr. 2010.
- [14] S. Amari, U. Rosenberg, and J. Bornemann, "Adaptive synthesis and design of resonator filters with source/load-multiresonator coupling," *IEEE Trans. Microw. Theory Tech.*, vol. 50, pp. 1969-1978, 2002.

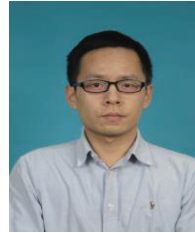


Dao Tong Li received the B.S. degree in Electronic Information Science and Technology from Binzhou University, Binzhou, China, in 2010. He is currently working toward the Ph.D. degree in the School of Electronic Engineering, University of Electronic Science and Technology of China (UESTC), Chengdu, China. His research interests include RF/microwave and mm-wave devices, circuits and systems.



Yong Hong Zhang received the B.S., M.S. and Ph.D. degrees from the University of Electronic Science and Technology of China (UESTC), Chengdu, China, in 1992, 1995, and 2001, respectively. He is currently a Full Professor in the School of Electronic Engineering,

University of Electronic Science and Technology of China. His research interests are in the area of microwave and millimeter wave technology and applications.



Kai Da Xu received the B.S. and Ph.D. degrees in Electromagnetic Field and Microwave Technology from the University of Electronic Science and Technology of China (UESTC), Chengdu, China, in 2009 and 2015, respectively. He is now an Assistant Professor with the Institute of Electromagnetics and Acoustics, and Department of Electronic Science, Xiamen University, Xiamen, China. His research interests include RF/microwave and mm-wave circuits, antennas, and nanoscale memristors.



Kai Jun Song received the M.S. degree in Radio Physics and the Ph.D. degree in Electromagnetic Field and Microwave Technology from the University of Electronic Science and Technology of China (UESTC), Chengdu, China, in 2005 and 2007, respectively. Since 2007, he has been with the EHF Key Laboratory of Science, School of Electronic Engineering, UESTC, where he is currently a Full Professor. His current research fields include microwave and millimeter-wave/THz power-combining technology; UWB circuits and technologies; microwave/millimeter-wave devices, circuits and systems; and microwave remote sensing technologies.



Joshua Le-Wei Li received his Ph.D. degree in Electrical Engineering from Monash University, Melbourne, Australia, in 1992. In 2010, he was invited to join the School of Electronic Engineering at the University of Electronic Science and Technology of China (UESTC), Chengdu, China. His research interests include electromagnetic theory computational electromagnetics, radio wave propagation and scattering in various media, microwave propagation and scattering in tropical environment, and analysis and design of various antennas.